Hindawi
Shock and Vibration
Volume 2018, Article ID 1402697, 9 pages
https://doi.org/10.1155/2018/1402697

*Research Article*

# Experimental Analysis of an Active Vibration Frequency Control in Gearbox

**Han Wang, Feng Zhang, Haiyan Li, Wenhao Sun, and Shunan Luo**

*College of Mechanical Engineering and Automation, Huaqiao University, Xiamen, Fujian 361021, China*

Correspondence should be addressed to Feng Zhang; zhangfeng@hqu.edu.cn

Received 12 April 2018; Accepted 10 July 2018; Published 9 September 2018

Academic Editor: Marc Thomas



Aiming at the vibrations of the multistage gear transmission system aroused by the gear meshing excitation, a novel active vibration control structure with built-in piezoelectric actuators (PZT) was established. The active control forces generated by the PZT were transmitted to the shafts through the additional supporting bearings. In addition, an adaptive fuzzy proportion integration differentiation (AFPID) control algorithm was proposed as the primary control algorithm to reduce the transverse vibrations of the gear shaft. According to the control law of PID parameters, a fuzzy inference module was designed to adaptively adjust the PID parameters to obtain the optimal control effect. An experimental platform was set up to verify the control effect of the algorithm. The experiments performed show 10 dB reduction in housing vibrations at certain targeted mesh harmonics over a range of operating speeds.

## 1. Introduction

The gear system is the most widely used mechanical transmission system. With the continuous development of aviation, aerospace, and robotics, the requirements for gear accuracy, gear vibration, and noise are becoming more rigorous. Due to the effects of nonlinear factors such as gear machining errors, installation errors, time variation of gear stiffness, external load changes, and meshing impact, the meshing relationship of the gear transmission system is destroyed, and the gear meshing position is shifted relative to the theoretical position, making the instantaneous transmission ratio changing, resulting in the collision between teeth and teeth, forming the error excitation of the gear meshing, thereby generating vibration [1].

The internal excitation of the gear transmission system is periodic. The vibration energy generated is mainly concentrated on the gear mesh frequency and its harmonic frequencies. As a new vibration control method is developed in recent years, the vibration active control which is based on the vibration signal obtained by the sensor generates a vibration signal to neutralize the harmful vibration. The generated vibration signal is equal to the vibration source and in the opposite direction [2]. Scholars have started to study for a long time. The concept of active control was proposed extremely early, and it was first applied to active noise control. In the 1930s, Paul [3] proposed to use active noise cancellation method instead of passive noise control, using a sensor to generate a secondary interference to the system, offset the existing primary noise, so that the initial noise was attenuated. But the control effect was limited by the control theory at the time and the limitations of electronic control devices. Until the early 1980s, Swigert studied the cylindrical antenna model control using piezoelectric ceramic components, creating a precedent for using intelligent structures to active vibration control. Montague et al. [4] is one of the first researchers to study the active vibration control of gear transmission systems. They applied a piezoelectric actuator on the gearbox drive shaft as a new type of gear vibration control method. The experimental results showed that only the basic frequency of the vibration of the gearbox was controlled and the desired excitation signal can be obtained only by adjusting the phase shifter and the amplifier manually. Rebbechi et al. [5] used two sets of magnetostrictive actuators to act on the bearings and applied an adaptive controller to control the actuator to suppress the vibration of the gear shaft and the box. The experimental results showed the vibrations of the meshing frequency, and second-order and third-order harmonic frequencies were reduced. Guan et al. [6] proposed to use a single piezoelectric actuator to construct an active gear control structure. The active control force of the actuator was applied to suppress the gear meshing vibration. The experimental results showed that the vibration at the target harmonic frequency was obvious attenuated. Li et al. [7] constructed a gear active structure with a piezoactuator attached to the gear shaft of a single-stage transmission system. The active control was performed using the FxLMS algorithm. The results showed that the vibration of the drive system reduced 6.9 dB at the meshing frequency. Fan [8] designed a single-stage gear transmission system and built a vibration active control platform, using PID control and fuzzy control as the controller. The experiment showed that the vibration of the gear system was significantly weakened. Dogruer and Pirsoltan [9] designed a nonlinear controller that could adjust the torque acting on the input shaft gear, which could effectively reduce the impact caused by the time-varying meshing stiffness.

The above studies mainly focused on the active control of single-stage gear transmissions, and the vibration coupling of multistage gears is more complicated. In addition to the single-axis mode and the interaxis coupling mode, new models are derived, resulting in a mode distribution. The vibration excitation of the high-speed shaft not only stimulates the high vibration of the shaft but also excites the vibration of other shafts. To verify the effectiveness of this active control in suppressing vibration during gear transmission, dynamic modelling of the gear transmission system was carried out to establish a virtual prototype. In addition, in the MATLAB/Simulink platform, the AFPID algorithm was used to carry out the multiharmonic vibration active control cosimulation of the gear transmission system.

## 2. Gear System Transmission Model

Gear machining errors, time variation of gear stiffness, changes in external loads, meshing impacts, and other factors can affect the meshing of gear drives [10]. Adding a control force near the excitation source can effectively reduce the meshing excitation. A gear drive active control structure with a built-in piezoelectric actuator is designed, as shown in Figure 1. The speed-regulating drive motor meets the requirements of large adjustable speed range and small speed fluctuation. The dynamometer consists of magnetic powder brake and torque sensor [11]. Through the design and verification of the transmission system, the basic data of all levels of gears are obtained, as shown in Table 1.

The piezoelectric actuator is a device that utilizes the inverse piezoelectric effect of piezoelectric ceramics to convert electrical energy into mechanical energy. It has the advantages of high control accuracy and fast response speed, which is widely used in precision positioning, position compensation, and active vibration control. Figure 2 is an enlarged view of the inside of the active control mechanism. The piezoelectric actuator support set is composed of an actuator bracket, an antiloading rod, and a support bearing. The antiloading rod has a certain degree of flexibility, which can play a role of overload protection function. The actuator bracket is fixed inside the box. And the end of the actuator is fixed on the actuator bracket for limiting its movement. A support bearing is added at the connection between the front of the actuator and the gear shaft. The actuator outputs a control force for the radial vibration of the gear shaft so as to attenuate the bending vibration of the gear shaft.

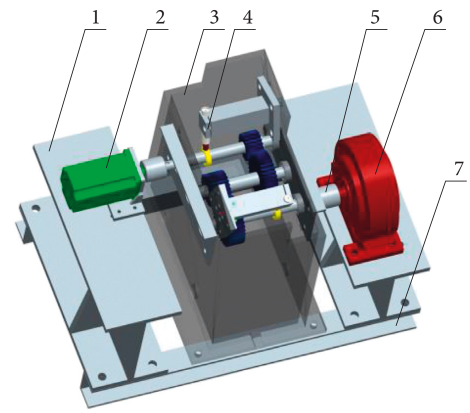


Figure 1: Gear drive active control system with a built-in piezoelectric actuator. (1) Bracket. (2) Adjustable speed motor. (3) Gearbox. (4) Piezoelectric actuator. (5) Coupling. (6) Magnetic powder brake. (7) Gearbox base.

Table 1: Gear parameters at all levels.

| Part name | Teeth | Modulus (mm) | Pressure angle (°) |
|---|---|---|---|
| High-speed shaft gear | 19 | 2.0 | 20 |
| Low-speed shaft gear | 35 | 2.0 | 20 |
| Intermediate shaft big gear | 37 | 2.0 | 20 |
| Intermediate shaft small gear | 23 | 2.0 | 20 |

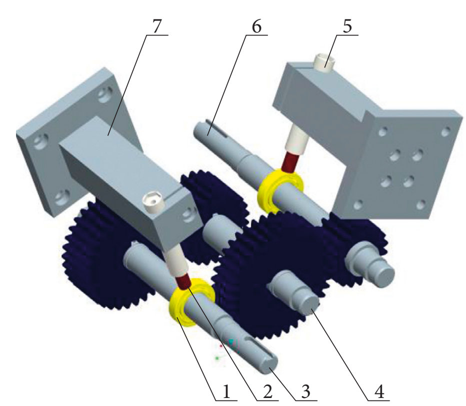


Figure 2: A detailed view of the internal structure of active control. (1) Support bearing. (2) Antiloading rod. (3) Output shaft. (4) Intermediate shaft. (5) Piezoelectric actuator. (6) Input shaft. (7) Actuator bracket.

The collision force in ADAMS software is defined as

$$F = \mathrm{MAX}\left\{0, K\left(q_0 - q\right)^e - C \times \left(\frac{dq}{dt}\right) \times \mathrm{STEP}\left(q,\, q_0,\, d,\, 1,\, q_0,\, 0\right)\right\}, \tag{1}$$

where $q_0$ is the initial distance between the two objects, $q$ is the actual distance during the collision of the two objects, and $q_0 - q$ is the deformation during the collision.

When $q \geq q_0$, that is, the two objects did not collide, and the collision force value is zero. When $q < q_0$, the two objects collided. The magnitude of the collision force is related to the stiffness coefficient $K$, the deformation quantity $q_0 - q$, the collision index $e$, the damping coefficient $C$, and the deformation distance $d$ when the damping works completely.

Hertz contact theory shows that the gear crash stiffness coefficient is

$$K = \frac{4}{3} R^{1/2} E^*. \tag{2}$$

Relative radius of curvature $R$ is

$$\frac{1}{R} = \frac{1}{R_1} + \frac{1}{R_2}, \tag{3}$$

where $R_1$ and $R_2$ are the equivalent radii of the contact points of the two meshing gears, respectively:

$$\frac{1}{E^*} = \frac{1 - v_1^2}{E_1} + \frac{1 - v_2^2}{E_2}. \tag{4}$$

Since both pairs of gears are made of steel, their Poisson's ratio $v_1 = v_2 = 0.27$ and Young's modulus of the gear material $E_1 = E_2 = 2.07e + 11\,\mathrm{Pa}$. Combining with the data in Table 1, the high-speed gear's impact stiffness coefficient $K_{\mathrm{H}}$ could be calculated, $K_{\mathrm{H}} = 5.27e + 5N\,\mathrm{mm}^{3/2}$. And the low-speed gear's impact stiffness coefficient $K_{\mathrm{L}} = 5.54e + 5N\,\mathrm{mm}^{3/2}$. The change of force during the impact is mainly controlled by the spring. The energy absorbed by the damper is a small part of the total collision energy. So the damping coefficient $C$ is generally small, and the damping coefficient is $C = 50{\cdot}S^{-1}$ mm, collision index $e = 1.5$, and penetration depth $d = 0.1$ mm. The dynamic friction coefficient is 0.05, and the static friction coefficient is 0.08.

In order to prevent sudden changes in rotation speed when starting up, the STEP function was used to increase the rotation speed to 2500 r/min within 0.1 s, that is, STEP(time, 0, 0 d, 0, 1, 15000 d). Add a load torque to the output shaft: $1e + 3N$ mm.

The gear shaft should be made flexible, and the flexible shaft processing in the ADAMS platform is different from Ansys. A rigid shaft is separated into a number of flexibly connected short rigid shafts to create an offline flexible connector, the essence of which is still a rigid body.

In the ADAMS platform, aiming at the relationship between the components of the built-in multistage gear transmission system model, the corresponding constraints are added. Finally, a virtual prototype of the gear transmission system is obtained.

## 3. AFPID Control Algorithm

The AFPID control algorithm designed in this paper is an algorithm with higher precision control based on the PID control, which makes up for the shortcomings that the classical PID control cannot adjust the parameters in real time. The fuzzy controller adjusts the parameter increment of the PID control to improve the overall control performance. Therefore, the main task of the algorithm is to adjust the relationship between the three parameter increments $\Delta K_{\mathrm{p}}$, $\Delta K_{\mathrm{i}}$, and $\Delta K_{\mathrm{d}}$ and the error $e(t)$ and the error rate $\dot{e}(t)$. Quantification factors and proportion factors could be online adjusted, so that they maintain a suitable value, so as to obtain a reasonable output parameters, continue to detect $e(t)$ and $\dot{e}(t)$. Through the fuzzy control rule, the control period of the three parameter increments is continuously adjusted online, and the online self-tuning of the PID parameters in the control system is completed. As shown in Figure 3, on the basis of PID algorithm, the calculation of error and error rate of change is added. By searching the corresponding fuzzy inference matrix in the knowledge base and adjusting the parameters, the values of the three control components of proportional, integral, and differential are obtained. The gain in each control cycle is transferred to the PID controller to realize the adaptive control and automatically complete the optimal setting of the PID parameters so as to effectively obtain the optimal control parameters.

The designed AFPID controller is shown in Figure 3. It is a controller with two inputs ($e(t)$and$\dot{e}(t)$) and three outputs ($\Delta K_{\mathrm{p}}$ $\Delta K_{\mathrm{i}}$ and$\Delta K_{\mathrm{d}}$ ) . The vibration acceleration error is

$$e(t) = x(t) - y(t). \tag{5}$$

The error $e(t)$ and the error derivative $\dot{e}(t)$ enter the fuzzy controller. After the derivation of the fuzzy rules, the proportional coefficient increment $\Delta K_{\mathrm{p}}$, the integral coefficient increment $\Delta K_{\mathrm{i}}$, and the differential coefficient increment $\Delta K_{\mathrm{d}}$ are shown as:

$$\begin{aligned} K_{\mathrm{p}} &= K_{\mathrm{p1}} + \Delta K_{\mathrm{p}}, \\ K_{\mathrm{i}} &= K_{\mathrm{i1}} - \Delta K_{\mathrm{i}}, \\ K_{\mathrm{d}} &= K_{\mathrm{d1}} - \Delta K_{\mathrm{d}}. \end{aligned} \tag{6}$$

As a result, the output of the controller is

$$y(t) = K_{\mathrm{p}} e(t) + K_{\mathrm{i}} \int_0^t e(t)\,dt + K_{\mathrm{d}} \dot{e}(t). \tag{7}$$

The operation of the fuzzy controller has three main parts, namely, fuzzification, fuzzy inference, and defuzzification.

*3.1. Fuzzification.* Fuzzification is the process of converting real values into linguistic variables. The variation range of the acceleration error $e(t)$ and the error rate of change $\dot{e}(t)$ is defined as the domain of the fuzzy set:

$$e(t), \dot{e}(t) = \{-2, -1, 0, 1, 2\}. \tag{8}$$

Its fuzzy set is {NB, NS, ZE, PS, PB}. The fuzzy set can be represented by the membership function. They represent

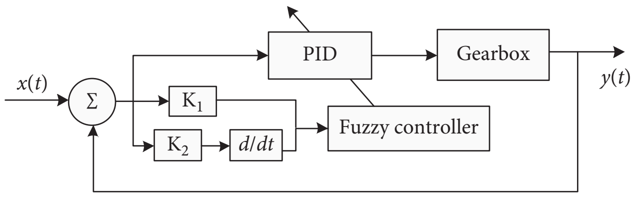


FIGURE 3: Flowchart of AFPID control algorithm.

negative big, negative small, zero, positive small, and positive big.

In the fuzzy design, the core is the selection of membership function. The curve of the membership function is adjusted according to the vibration environment. When the deviation is small, the density of the curve is increased. When the deviation is large, the density of the curve is reduced, which is helpful to improve the system's response accuracy and reduce overshoot. As shown in Figures 4–6, the classic membership functions are triangular, Gaussian, trapezoid, and other functional forms. The best membership function will be selected in the following simulation experiments, and the curve density will be adjusted.

*3.2. Design of Fuzzy Rules.* As a fuzzy language information processing system, fuzzy rules are divided into several types because of different control forms. The most common ones are Mamdani type and TS type. Mamdani-type fuzzy rules output fuzzy quantities, while TS-type fuzzy rules output a function. Therefore, the Mamdani-type fuzzy rules are more suitable as rules for language variable description [12]. This article uses Mamdani type to establish fuzzy control rules.

The design of fuzzy rules based on expert experience determines the optimal fuzzy rules by a large number of experiments. For the selection of the number of control rules, very few quantities will seriously affect the control effect, and too many quantities will increase the amount of computation and increase the experimental delay. Table 2 shows the inference rules of the fuzzy controller.

*3.3. Defuzzification.* Defuzzification, in contrast to fuzzification, is a method of converting linguistic variable values into real values. Since the result of fuzzy rule inference is a fuzzy set, it cannot be directly used as the control amount of the controlled object, and it needs to be turned into an accurate amount that can be executed [13]. The purpose of the solution is to get the best reflection of the control based on the result of fuzzy inference and the actual distribution of the quantity. The most common method is the centroid method which uses the center of gravity of the fuzzy membership function curve and the abscissa enclosing area as the final output value of the fuzzy reasoning. Since it has a smooth output inference rule, the centroid method is effective to determine a final output value of the fuzzy inference. There are other methods of defuzzification such as the median method and the maximum method.

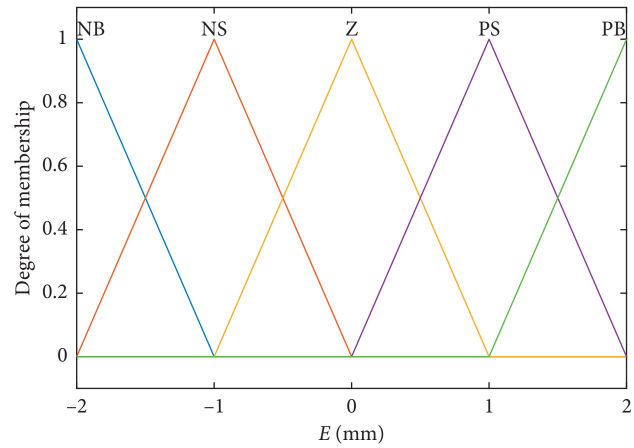


FIGURE 4: Triangular membership function.

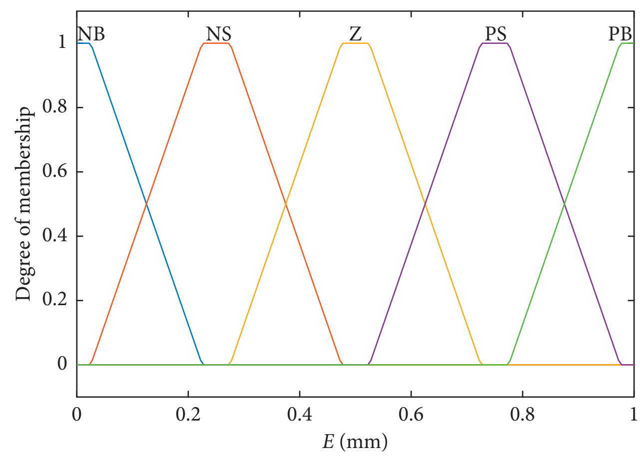


FIGURE 5: Trapezoid membership function.

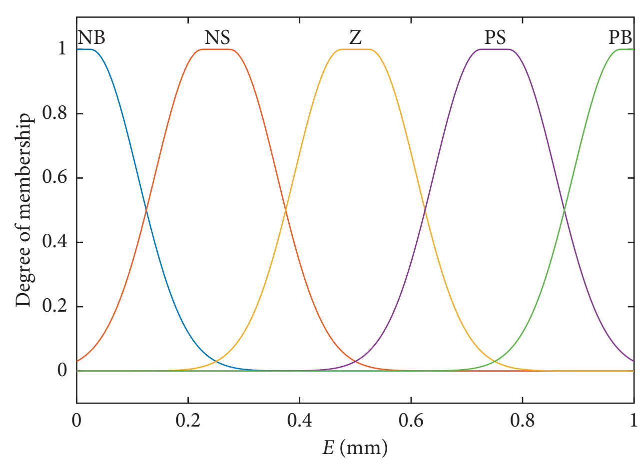


FIGURE 6: Gaussian membership function.

## 4. Simulation Comparison Analysis

ADAMS is an application software not only for analyzing virtual prototypes, but also can provide multiple parameterized modules with stronger functions, so it can be used as a secondary development tool platform.

Table 2: Fuzzy rules for $K_p$, $K_i$, and $K_d$.

| E | EC | | | | |
|---|---|---|---|---|---|
| | NB | NS | ZO | PS | PB |
| NB | PB/NB/PS | PB/NB/ZO | PB/NB/ZO | PS/NB/ZO | ZO/ZO/PS |
| NS | PB/NB/NB | PS/NB/NB | PS/NS/NS | ZO/NS/ZO | NB/ZO/PS |
| ZO | PS/NS/NB | PS/NS/NB | ZO/ZO/NS | NS/PS/ZO | NB/PS/PS |
| PS | PS/NS/NB | ZO/ZO/NS | NS/PS/NS | NS/PS/ZO | NB/PB/PS |
| PB | ZO/ZO/PS | NS/PS/ZO | NS/PS/ZO | NB/PB/ZO | NB/PB/PS |

The joint simulation of ADAMS and MATLAB establishes a virtual prototype of the gear transmission in ADAMS, making it a module with system equations and related parameters, as shown in Figure 7. In MATLAB, the data in the module are combined with the established control algorithm. The system equations are solved by ADAMS, and the MATLAB solves the control equations to complete the entire simulation process.

The speed is set to 2070 r/min, the load is set to 1000 N·mm, and the vibration signal of the gearbox is collected. As shown in Figure 8, the vibration signal extreme values are obtained at 407.3 Hz, 654.8 Hz, 815.5 Hz, 1223 Hz, and 1630 Hz. Among them, 407.3 Hz and 654.8 Hz are the meshing frequencies of the two pairs of gear shafts, respectively.

The AFPID algorithm is introduced into the active control system. Figure 9 shows the active control cosimulation of the multistage gear transmission system based on AFPID control. The fuzzy controller is the core of the algorithm. In addition to the establishment of inference rules, the choice of membership functions and defuzzification methods also greatly affect the control performance, as shown in Figures 10 and 11.

From the frequency domain diagram, it can be seen that the three membership functions and the defuzzification methods effectively reduce the vibration of the gear transmission system. The amplitude of the vibration at the main frequency is shown in Tables 3 and 4.

It can be seen from the table that the AFPID algorithm can obtain the best control effect by using the trapezoidal membership function and the centroid method in defuzzification. Experiments are carried on with the conventional PID control under the same condition. Figures 12 and 13 show the active control cosimulation of PID control.

From the time-domain diagram, it can be seen that both control methods effectively reduce the vibration of the gear transmission system, and the AFPID control has a better control performance. From the frequency domain diagram, it can be found that the gear system has the largest vibration energy distribution at the meshed fundamental frequency and the harmonic frequencies, while the amplitudes at the main frequencies of the PID control and the AFPID control both significantly are reduced.

From Table 5, it can be seen that the AFPID control is better than the classic PID control for the control performance of the gear mesh frequency and harmonic frequencies. When the speed is 2028 r/min, the gear transmission system has the greatest vibration at the third harmonic. AFPID control reduces vibration by 7.6 dB, reducing vibration by 7%.

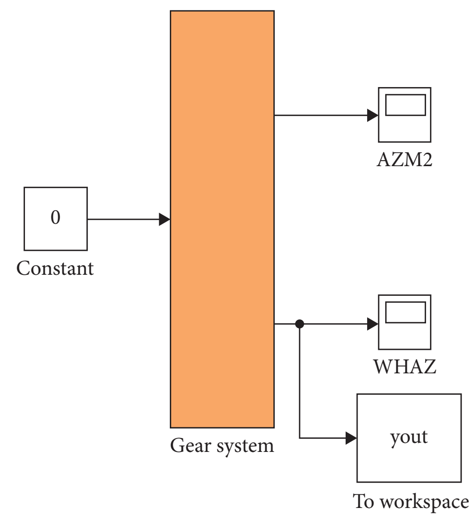


Figure 7: Acquisition of vibration signal before control.

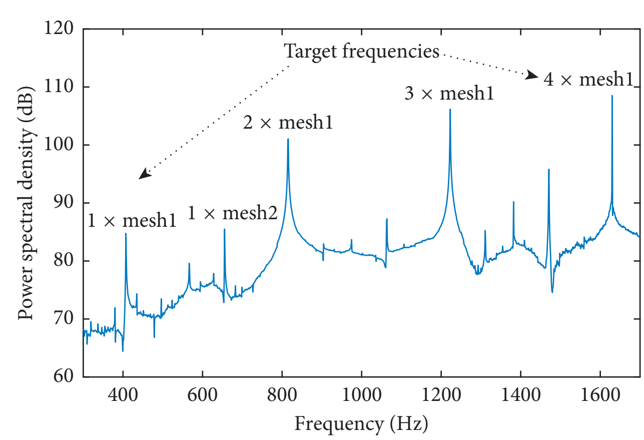


Figure 8: Vibration signal of gear system.

## 5. Experiment Analysis

Designing and building a multistage gear train vibration active control test platform mainly includes the following three parts: active control structure, control system, and signal acquisition and processing system.

The active control structure has been described in detail in the previous article. This article selects the RapidECU-S1

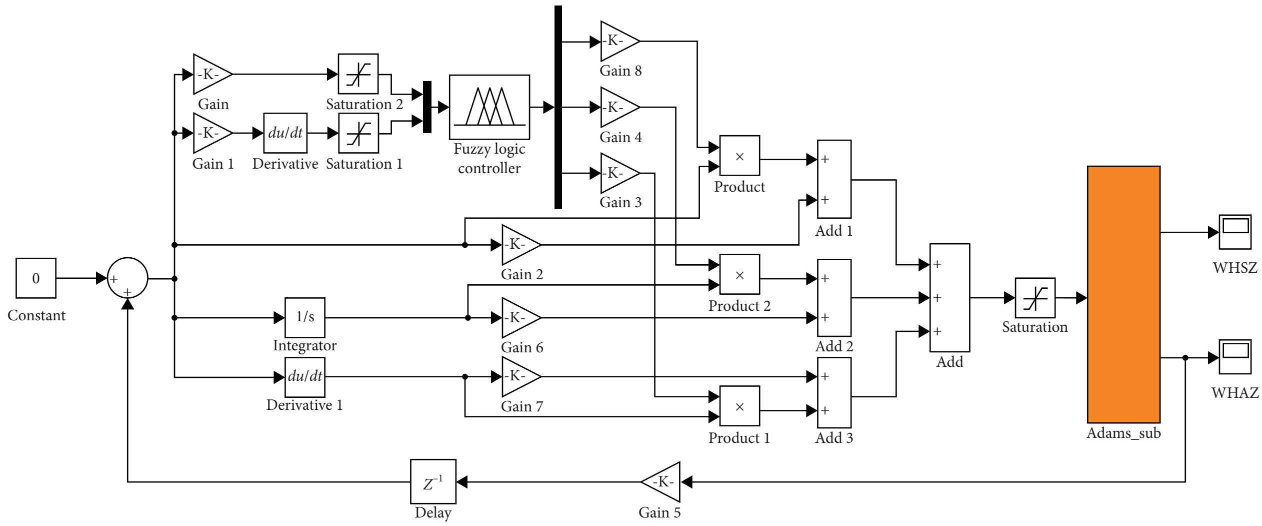


Figure 9: Cosimulation of active control of multistage gear transmission system based on AFPID control.

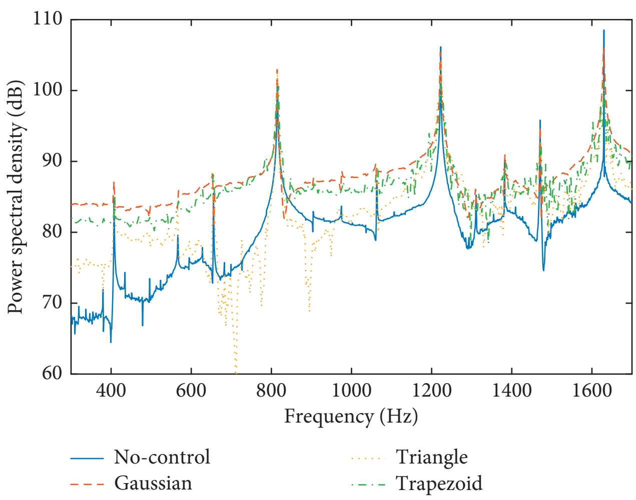


Figure 10: Frequency domain vibration active control of gear system based on different membership functions.

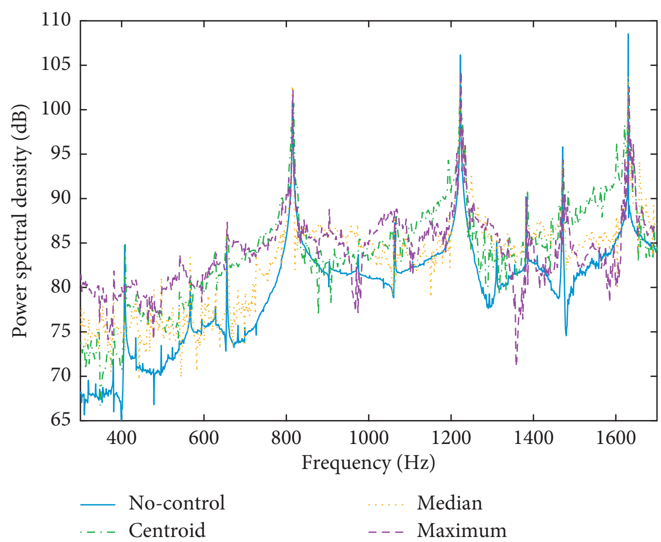


Figure 11: Frequency domain vibration active control of gear system based on different defuzzification methods.

real-time control simulation system as the vibration active control system and establishes the semiphysical simulation control platform. The software ECUcoder that matches the RapidECU-S1 can automatically generate the target code on the PC's control algorithm. Therefore, on the one hand, the control system receives the vibration signal of the gearbox collected by the vibration acceleration sensor. On the other hand, the control voltage signal is sent out in real time, the signal is adjusted by the control algorithm, and the piezoelectric actuator is driven to act on the transmission shaft to suppress the vibration of the system.

In order to observe the control performance during the experiment, it is necessary to process the collection results in real time and adjust the control parameters in real time. This section establishes a special collection and processing system. This system consists of four parts: a vibration acceleration sensor, a signal conditioner, a signal collector, and a PC. The vibration acceleration sensor is installed on the gearbox. The collected vibration acceleration signal is amplified by the signal conditioner and then collected and processed by the signal collector.

Table 3: The amplitudes of the system at the main frequencies based on different membership functions.

| Membership functions | Frequency (Hz) | | | | |
|---|---|---|---|---|---|
| | 407.3 | 654.8 | 815.5 | 1223 | 1630 |
| No-control | 84.75 | 85.85 | 101.1 | 106.2 | 108.5 |
| Trapezoid | 84.98 | 88.12 | 100.6 | 101 | 100.9 |
| Triangle | 83.03 | 85.50 | 102.3 | 104.5 | 102.0 |
| Gaussian | 87.16 | 88.30 | 103.0 | 105.4 | 105.1 |

Figure 14 is a complete vibration active control experiment platform. The two piezoelectric actuators are, respectively, fastened by additional supporting devices and act on the input shaft and the output shaft. The angle between the

Table 4: The amplitudes of the system at the main frequency based on different solution fuzzy methods.

| Defuzzification | Frequency (Hz) | | | | |
|---|---|---|---|---|---|
| | 407.3 | 654.8 | 815.5 | 1223 | 1630 |
| No-control | 84.75 | 85.85 | 101.1 | 106.2 | 108.5 |
| Centroid | 84.98 | 88.12 | 100.6 | 101 | 100.9 |
| Median | 76.27 | 86.61 | 102.7 | 103.4 | 103.7 |
| Maximum | 80.26 | 87.37 | 102.2 | 104.3 | 102.6 |

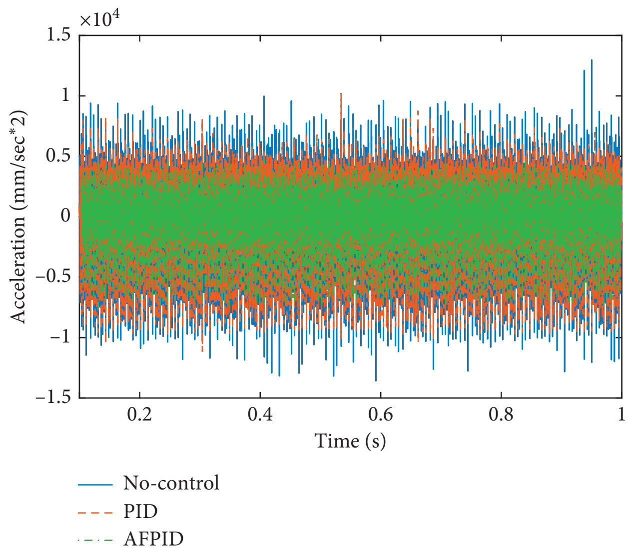


Figure 12: Active control of vibration in the time domain of gear transmission system.

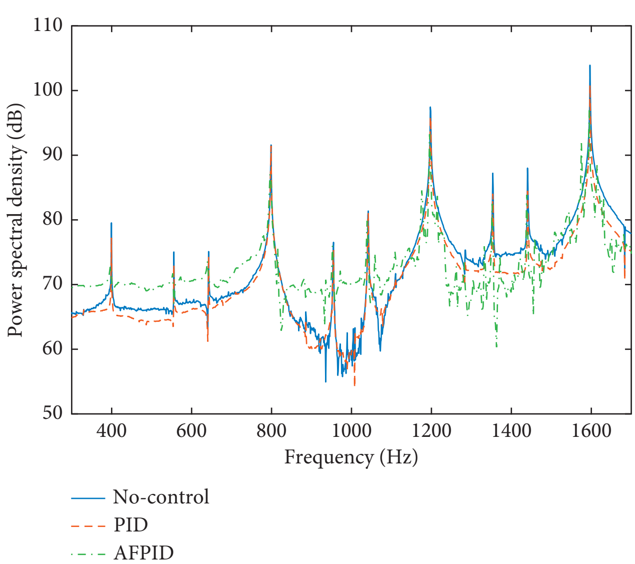


Figure 13: Active control of vibration in the frequency domain of gear transmission system.

axis direction of the piezoelectric actuator and the vertical direction is 20°; that is, it is ensured that the control force line coincides with the direction of the meshing line of the gear transmission. The signal conditioning is connected to the

Table 5: The amplitudes of the vibration of the gear system at the main frequencies.

| Control method | Frequency (Hz) | | | | |
|---|---|---|---|---|---|
| | 407.3 | 654.8 | 815.5 | 1223 | 1630 |
| No-control | 84.75 | 85.85 | 101.1 | 106.2 | 108.5 |
| PID control | 83.84 | 85.65 | 101.4 | 105.7 | 106.8 |
| AFPID control | 84.98 | 88.12 | 100.6 | 101 | 100.9 |

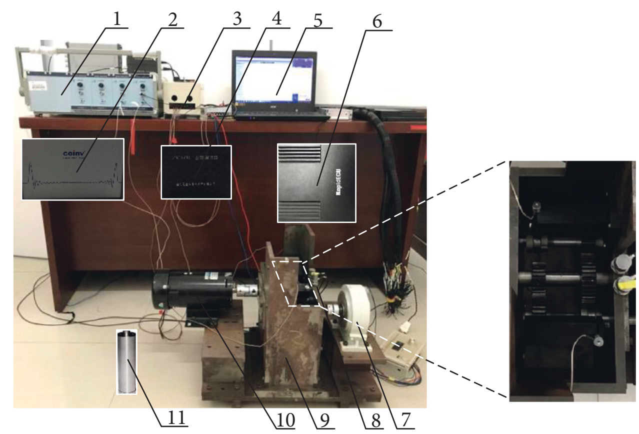


Figure 14: Gear system vibration active control test platform. (1) Power amplifier. (2) Signal collector. (3) Motor governor. (4) Signal conditioner. (5) Computer. (6) Real-time simulation system. (7) Magnetic powder brake. (8) Vibration acceleration sensor. (9) Gearbox. (10) Drive motor. (11) Piezoelectric actuator.

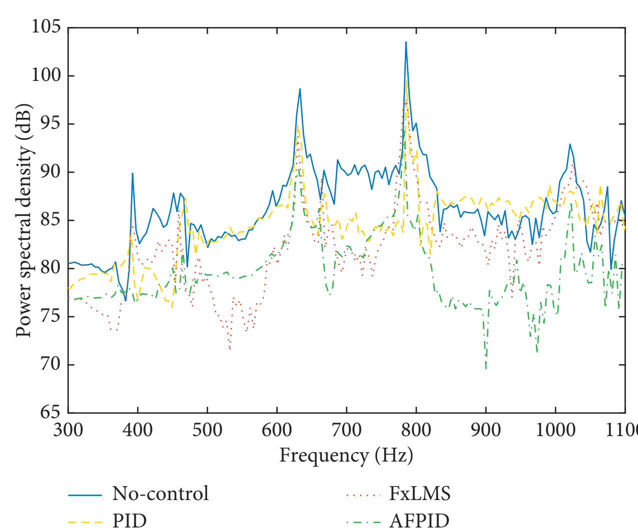


Figure 15: Frequency domain diagram of active gearbox vibration control.

sensor, and the power amplifier is connected to the piezoelectric stack actuator. The vibration acceleration sensor is the input of the signal collector, and the measured vibration acceleration signal is used as a judging index of the box vibration; another vibration acceleration sensor is located close to the output of the actuator as an input signal to the control system.

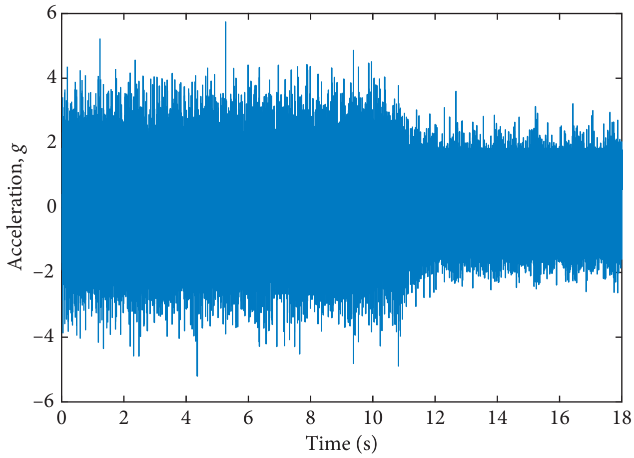


Figure 16: Time-domain diagram of gearbox vibration active control.

The speed of the drive motor is adjusted to 2000 r/min, and the load of the magnetic powder brake is adjusted to 1 Nm. The vibration acceleration signal of the gearbox collected by the signal collector is shown in Figure 15. Among them, the most obvious vibration acceleration peaks are generated at 633 Hz and 787 Hz. They are all meshing frequencies of the two pairs of gears.

Figure 16 shows the time-domain control history at 2000 r/min, and the control is turned on at the 10th second. It can be seen from the time-domain diagram that the vibration acceleration signal is significantly reduced in two seconds. The AFPID algorithm successfully suppresses the vibration of the gearbox and has obvious control effects. Figure 15 shows the frequency domain diagram of the active vibration control of the gearbox under different algorithms, such as classical PID control and FxLMS control. Experimental results clearly show that AFPID algorithm has better control effect. The vibration of the gear after control has been weakened to a certain degree. The vibration at the 787 Hz is reduced by 10 dB. The vibration at the other frequencies is obviously reduced.

## 6. Conclusions

In order to control the vibration and noise caused by the internal excitation of the gear transmission system, this paper constructs an experimental platform for active vibration control of the gear actuator system with built-in piezoelectric actuators. The active control algorithm of AFPID is used to carry out the experimental study of active vibration control. The following conclusions are obtained:

(1) It could be found that the gear system has the largest vibration energy distribution at the meshed fundamental frequency and the harmonic frequencies. The experimental study confirms the correctness of the active vibration control structure.

(2) Through the comparative analysis in the cosimulation, the trapezoidal membership function and the centroid solution selected to make the AFPID algorithm have the productive control effect. The experiments performed show 10 dB reduction in housing vibrations at harmonic frequencies.

## Data Availability

The vibration of the gearbox with no-control data used to support the findings of this study have been deposited in the FAIRsharing.org repository. The vibration of the gearbox with AFPID data used to support the findings of this study are currently under embargo while the research findings are commercialized. Requests for data, 12 months after publication of this article, will be considered by the corresponding author.

## Conflicts of Interest

The authors declare that there are no conflicts of interest regarding the publication of this paper.

## Acknowledgments

This study was supported by the National Natural Science Funds (51405169).

## References

[1] Y. Li, K. Ding, G. He et al., "Vibration mechanisms of spur gear pair in healthy and fault states," *Mechanical Systems and Signal Processing*, vol. 83, pp. 183–185, 2016.

[2] Z. Zhang, J. Wang, J. Zhou et al., "Adaptive vibration control based on tracking filter," *Journal of Vibration and Shock*, vol. 28, no. 2, pp. 64–67, 2009.

[3] L. Paul, "Process of silencing sound oscillation," US Patent 2043416, 1936.

[4] G. T. Montague, A. F. Kascak, A. Palazzolo et al., "Feedforward control of gear mesh vibration using piezoelectric actuators," *Shock and Vibration*, vol. 1, no. 5, pp. 473–484, 1994.

[5] B. Rebbechi, C. Howard, and C. Hansen, "Active control of 00 gearbox vibration," in *Proceedings of the Active Control of Sound and Vibration Conference*, pp. 295–304, Fort Lauderdale, FL, USA, 1999.

[6] Y. H. Guan, T. C. Limb, and S. W. Shepard, "Experimental study on active vibration control of a gearbox system," *Journal of Sound and Vibration*, vol. 282, no. 3–5, pp. 713–733, 2005.

[7] Y. Li, F. Zhang, Q. Ding et al., "Active control method and experimental study of gear meshing vibration," *Journal of Vibration Engineering*, vol. 27, no. 2, pp. 215–221, 2014.

[8] Z. Fan, *Research on Active Control of Bending Vibration of Spur Gear Drive*, Chongqing University, Chongqing, China, 2010.

[9] C. U. Dogruer and A. K. Pirsoltan, "Active vibration control of a single-stage spur gearbox," *Mechanical Systems and Signal Processing*, vol. 85, pp. 429–444, 2017.

[10] Y. Li, F. Zhang, L. Wang et al., "Active vibration control of gear meshing based on on-line identification of secondary channels," *Vibration and Shock*, vol. 32, no. 16, pp. 7–12, 2013.

[11] H. Wang, F. Zhang, H. Li et al., "Multi-stage gear vibration active control based on AFPID control," in *Proceedings of International Conference on Advanced Mechatronic Systems*, Xiamen, China, December 2017.

[12] A. M. Reza, S. Mohammad, K. T. Mahdi et al., "Observer-based adaptive fuzzy controller for nonlinear systems with

unknown control directions and input saturation," *Fuzzy Sets and Systems*, vol. 314, pp. 24–45, 2017.

[13] J. Dong and J. Hou, "Output feedback fault-tolerant control by a set-theoretic description of T–S fuzzy systems," *Applied Mathematics and Computation*, vol. 301, pp. 117–134, 2017.